Available online at www.sciencedirect.com
SCIENCE DIRECT®
Journal of Solid State Chemistry 179 (2006) 665–670
JOURNAL OF SOLID STATE CHEMISTRY
www.elsevier.com/locate/jssc

A one-dimensional zirconium hydroxyfluoride, $[Zr(OH)_2F_3][enH]$

Daniel P. Brennan[a], Peter Y. Zavalij[b], Scott R.J. Oliver[a,*]

[a]*Department of Chemistry and Biochemistry, University of California, 1156 High Street, Santa Cruz, CA 95064, USA*
[b]*Department of Chemistry and Biochemistry, University of Maryland, College Park, MD 20742, USA*

Received 20 August 2005; received in revised form 19 November 2005; accepted 20 November 2005
Available online 4 January 2006

Abstract

The first example of a unidimensional zirconium hydroxide fluoride was synthesized under mild solvothermal treatment and characterized by X-ray diffraction and thermal techniques. Monoprotonated ethylenediamine cations reside between the anionic chains. Crystal data for this material are as follows: $[C_2N_2H_9][Zr(OH)_2F_3]$, $M = 243.35$, orthorhombic, space group $Pca2_1$, $a = 6.8016(13)$, $b = 6.1393(12)$, $c = 14.867(3)$ Å, $V = 620.8(2)$ Å^3, $T = 294(2)$ K, $Z = 4$, $D_c = 2.604$ g cm^{-3}, μ(Mo-$K\alpha$) = 1.777 mm^{-1}, $\lambda = 0.71073$ Å. The material transforms to an unknown layered material at ~175 °C, a common occurrence for 1D structures where the chains are arranged in hydrogen-bonded layers and separated by interlayer organoammoniums. Collapse to the known condensed mineral phase $Zr(FO)_{2.7}$ occurs at ca. 275 °C before finally transforming to the baddeleyite form of ZrO_2 at ca. 460 °C.

Keywords: Zirconium-based chain; Zirconium hydroxyfluoride; Solvothermal synthesis; Ethylenediamine

1. Introduction

Organic amines have long been used as structure-directing agents in the solvothermal synthesis of extended materials. The majority of work on the templating of open zirconium-based compounds with organoammonium cations has focused on the formation of layered and open-framework phosphates [1,2] and fluorophosphates [3–5]. The zirconium phosphates have attracted particular attention due to their very rich intercalation chemistry and ion-exchange capability. In addition, ionic conduction in NASICON-type systems such as $Li_2Zr_2(PO_4)_3$ has been thoroughly studied in recent years [6,7]. Such applications require a relatively high degree of structural integrity, which explains the emphasis on 2D and 3D architectures.

Relatively little has been reported concerning low-dimensionality zirconium-based materials. A number of zirconium hydroxide nitrate hydrates possess 1D chain structures, determined by analysis of their powder X-ray diffraction (PXRD) data [8,9]. Only a handful of 1D zirconium fluoride hydrates have been published [10,11], and there are only three 1D zirconium phosphate materials known to date [12–14]. In addition, Clearfield and coworkers reported a linear chain zirconium phosphonate material [15]. Some recent work on the hydrolysis of fluorozirconate glasses has provided evidence for zirconium hydroxyfluoride species, but these solids are non-crystalline and characterized primarily by X-ray photoelectron spectroscopy (XPS) [16]. To our knowledge, 1D zirconium hydroxyfluoride chains have not been reported.

We have discovered a series of extended metal fluorides and phosphonates, where the dimensionality can be cluster, chain, layered or framework, and the metal is Ge, Sn or Pb [17–20]. In addition, these inorganic structures are anionic [17], neutral [18,19] or cationic [20]. For the fluoride-containing members of this series, the fluorides are either terminal, as in the case of an anionic tin fluorophosphate [17] and germanium tetrafluorobispyridine [18], or bridging, as for a neutral tin fluorophosphate [19] and cationic $Pb_3F_5(NO_3)$ [20]. Although fluoride can be bridging for larger metals such as Sn and Pb, it is often terminal for most metals, including zirconium.

We report here the synthesis and characterization of $[Zr(OH)_2F_3][enH]$, a 1D anionic structure which we denote SLUG-1 (University of California, Santa Cruz, structure

*Corresponding author. Fax: +1 831 459 2935.
E-mail address: soliver@chemistry.ucsc.edu (S.R.J. Oliver).

0022-4596/$ - see front matter © 2005 Elsevier Inc. All rights reserved.
doi:10.1016/j.jssc.2005.11.040

number 1). The material is composed of infinite zirconium hydroxide fluoride chains charge-balanced by monoprotonated ethylenediamine cations.

2. Experimental

2.1. Synthesis

The material was synthesized by solvothermal methods. All chemicals were purchased from Acros and used as-received. In a typical reaction, 4.88 g of isopropanol, 0.81 g of ethylenediamine (en) and 1.27 g of zirconium(IV) *n*-propoxide (70 vol% in *n*-propanol) were added to a Nalgene beaker. After stirring briefly, 0.48 g of tetrafluoroboric acid (50 mass% in water) and 1.46 g of distilled water were added. The final reaction mixture had a molar ratio of 30 H_2O:30 ^{i}PrOH:1 $Zr(O^{n}Pr)_4$: 5 $H_2N(CH_2)_2NH_2$ (en):1 HBF_4. The pH of the reaction mixture was 11.5. The resultant gel was homogenized for 5 min before it was transferred to a 23 ml capacity Teflon-lined stainless steel autoclave. The autoclave was sealed and heated at 398 K for 3 days, after which time a crop of crystals was visible in the autoclave. The pH of the mother liquor was 10.9. The crystals were recovered by vacuum filtration, rinsed with deionized water and acetone, and allowed to air-dry overnight (yield: 43.7%).

2.2. Characterization

PXRD data was acquired on a Scintag XDS 2000 diffractometer using a solid-state detector and Cu-$K\alpha$ radiation ($\lambda = 1.5418$ Å) over a scan range of 2–45° (2θ), a step size of 0.02° and a scan rate of 4.0° min^{-1}. A suitable colorless prism (approximate dimensions $0.32 \times 0.07 \times 0.06$ mm^3) was manually selected for single-crystal X-ray diffraction (SCXRD) analysis (Table 1). SCXRD was performed on a Bruker AXS single-crystal diffractometer with SMART Apex detector, using a graphite monochromator and a Mo-$K\alpha$ fine-focus sealed tube ($\lambda = 0.71073$ Å). Operating conditions were 50 kV and 40 mA, ω-scan, ω step size 0.30° and 10 s exposition time, with the detector placed at a distance of 5.171 cm from the crystal. The total time for data collection was 7.01 h.

The integration of the data using an orthorhombic unit cell yielded a total of 6296 reflections to a maximum θ angle of 28.28°, of which 1512 were independent (completeness = 99.6%, $R_{int} = 7.95\%$, $R_{sig} = 5.95\%$) and 1275 were greater than $2\sigma(I)$. The final cell dimensions of $a = 6.8016(13)$ Å, $b = 6.1393(12)$ Å, $c = 14.867(3)$ Å, $\alpha = 90°$, $\beta = 90°$, $\gamma = 90°$, $V = 620.8(2)$ Å^3, are based upon the refinement of the XYZ-centroids of 1744 reflections with $2.7° < \theta < 31.0°$ using SAINT. Analysis of the data showed 0.29% decay during data collection. Data were corrected for absorption effects with the semi-empirical from equivalents method using XPREP [21]. The minimum and maximum transmission coefficients were 0.645 and 0.899. The structure was solved and refined using the SHELXS-97 [22] and SHELXL-97 [23] software in the space group $Pca2_1$ with $Z = 4$ for the formula unit $[ZrF_3(OH)_2][enH]$. The final anisotropic full-matrix least-squares refinement on F^2 with 71 variables converged at $R_1 = 4.87\%$ for the observed data and $wR_2 = 11.16\%$ for all data.

Thermogravimetric analysis was performed on a TA 2950 under nitrogen flow, heating from room temperature to 600 °C at a rate of 5 °C min^{-1}. Solid-state nuclear magnetic resonance (NMR) analysis was performed on a Bruker AC 300. Fourier transform infrared spectroscopy (FTIR) spectra were acquired on a Bruker Equinox 55. Scanning electron microscopy (SEM) data was collected on a Hitachi S-570 SEM. Prior to analysis, the sample was coated with a 1:1 Au:Pd alloy in a Denton Vacuum Desk 1 sputter coater. SEM operating conditions were 15 kV accelerating voltage and 17 mm working distance. Elemental analysis was performed by Quantitative Technologies, Inc. (Whitehouse, NJ).

3. Results and discussion

The entire product after rinsing with water was fractal aggregates of needle-like crystals (average size ca. 400 μm × 70 μm × 50 μm, Fig. 1). The relatively low yield is due to the formation of a secondary solid product, which dissolves when rinsed with acetone and water. This secondary phase could not be identified as it readily decomposes in air. Attempts to isolate solely the title compound without production of this second phase by reducing the amount of fluoride (from tetrafluoroboric acid) were not successful. PXRD data (Fig. 2a) could not be matched to any known phase. Subsequent SCXRD of a manually selected crystal confirmed that the compound is indeed a new structure. The theoretical PXRD pattern

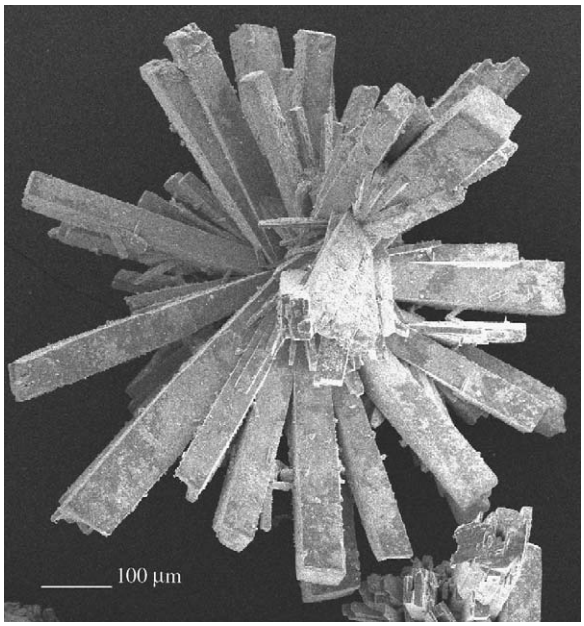

Fig. 1. SEM image of the fractal cluster morphology of SLUG-1 crystals.

calculated from the single-crystal data matched that of the as-synthesized product (Fig. 2a), verifying that the rinsed product is phase-pure.

The structure is composed of edge-sharing $Zr(OH)_4F_3$ pentagonal bipyramids, with both axial positions occupied by terminal fluoride ions (Fig. 3). To our knowledge, the $Zr(OH)_4F_3$ polyhedron has not been reported previously. The pentagonal plane consists of four bridging hydroxides and the remaining terminal fluoride ion. H atoms from the OH groups were located from difference maps and can be refined without any constraints. In the final refinement, the geometry was constrained but U_{iso} was refined, which confirms their presence. Another confirmation is the almost perfect hydrogen bonds the hydroxide protons make with the equatorial fluorides from neighboring chains. No reasonable peaks were detected at the other assigned fluoride atoms.

Due to the similarities in X-ray scattering and bond distances for F and OH, however, elemental analysis was performed to determine the sample's fluoride content. The %F was determined to be 23.30%, which is nearly identical to the theoretical value of 23.42% for the proposed structure. ^{19}F solid-state NMR was also performed to confirm the fluoride positions in the structure. Only two peaks were observed, consistent with a structure that possesses two F atoms in equivalent axial positions and a third F atom in the base of the pentagon. Finally, the presence of a broad peak in the IR spectrum at $\sim 3500\,cm^{-1}$ indicates the presence of hydroxide groups in the structure.

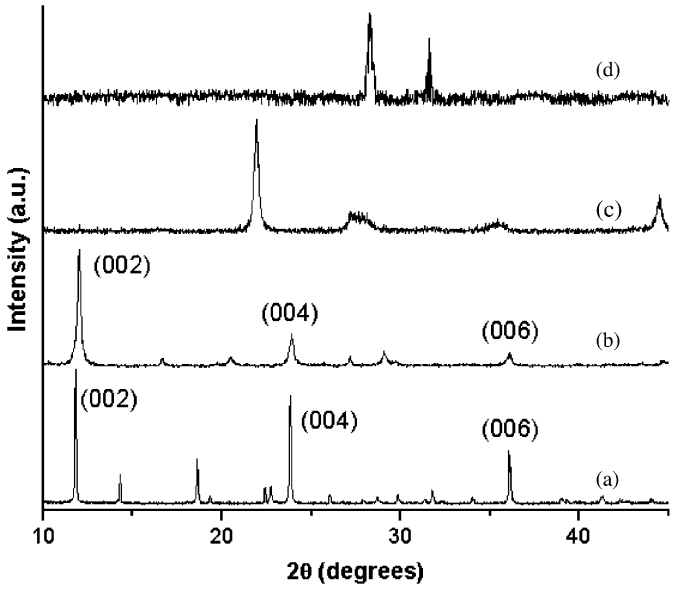

Fig. 2. PXRD data for the as-synthesized product (a) and after heating in air to 230 °C (b), 400 °C (c) and 600 °C (d).

The atom labeling scheme is given in Fig. 4. Alternate equatorial sides of the pentagonal bipyramids edge-share along the *a*-axis, creating a zig-zag chain structure (Fig. 3a). The structure also displays long Zr–Zr contacts (3.5918(7) Å, Table 2), in accordance with literature values [24]. Significant interchain hydrogen bonding interactions occur among the H atoms on the hydroxide groups and fluoride groups on neighboring chains (Table 3). The chains are charge-balanced by monoprotonated ethylenediamine cations that reside in the interchain voids (Fig. 3b). The cations are disordered with respect to the location of the amine group. Attempts to characterize the degree of template protonation by ^{13}C solid-state NMR were unsuccessful due to severe peak broadening by the structural fluorine atoms, making it impossible to obtain such information from these spectra. Bond valence sum calculation of the hydroxide groups on the zirconiums, however, support a monoprotonated form, as does the formula of the compound. Powell and co-workers have recently reported two layered structures also charge-balanced by monoprotonated ethylenediamine cations, although they did not report a direct method for determining the degree of protonation for either material [25].

Based on our observed structure, it is likely the inorganic connectivity was limited to one dimension by the presence of terminal fluoride groups at both the axial and one equatorial position. This termination of inorganic dimensionality often occurs, such as in the ammonium-templated anionic tin fluorophosphate we reported [17]. For the present compound, HBF_4 acted as fluoride source, and in

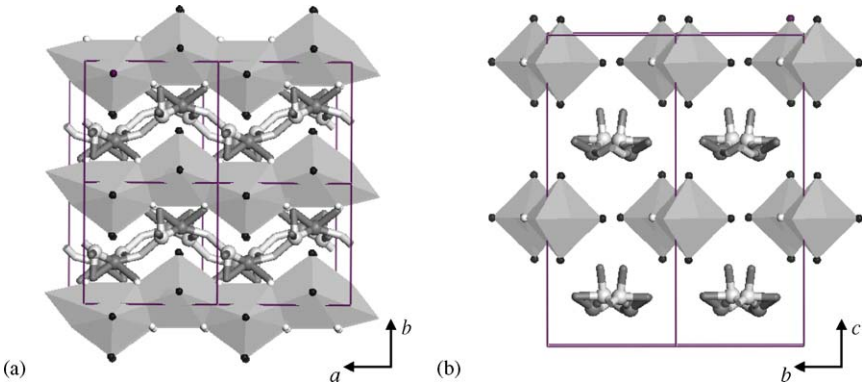

Fig. 3. Polyhedral views along the *c*-axis (a) and *a*-axis (b). Inorganic polyhedral shading scheme: Zr—centers of the gray polyhedra; O—white spheres; F—black spheres. Organic ball and stick shading scheme: C—light gray, N—dark gray. Hydrogens omitted for clarity.

Table 1
Data collection and structure refinement for $[Zr(OH)_2F_3][enH]$

Diffractometer	Bruker Smart Apex CCD area detector
Radiation source	Fine-focus sealed tube, Mo-$K\alpha$
Generator power	50 kV, 40 mA
Detector distance	5.171 cm
Detector resolution	8.33 pixel/mm
Total frames	1868
Frame size	512 pixel
Frame width	0.3°
Exposure per frame	10 s
Total measurement time	7.01 h
Data collection method	ω scans
θ range for data collection	1.37–28.28°
Index ranges	$-9\leqslant h\leqslant 9$, $-8\leqslant k\leqslant 8$, $-18\leqslant l\leqslant 19$
Reflections collected	6296
Independent reflections	1512
Observed reflection, $I>2\sigma(I)$	1275
Coverage of independent reflections	99.6%
Variation in check reflections	0.29%
Absorption correction	Semi-empirical from equivalents XPREP [21]
Max. and min. transmission	0.899 and 0.645
Structure solution technique	Direct
Structure solution program	SHELXS-97 [22]
Refinement technique	Full-matrix least-squares on F^2
Refinement program	SHELXL-97 [23]
Function minimized	$\Sigma w(F_o^2-F_c^2)^2$
Data/restraints/parameters	1512/71/90
Goodness-of-fit on F^2	1.020
Δ/σ_{max}	0.001
Final R indices	
R_1, $I>2\sigma(I)$	0.0487
wR_2, all data	0.1116
R_{int}	0.0795
R_{sig}	0.0595
Weighting scheme	$w=1/[\sigma^2(F_o^2)+(0.05P)^2+2.45P]$ $P=[\max(F_o^2,0)+2F_c^2]/3$
Absolute structure parameter	0(10)
Largest diff. peak and hole	1.145 and -1.253 e/Å^3

$R_1=\Sigma||F_o|-|F_c||/\Sigma|F_o|$, w$R_2=[\Sigma w(F_o^2-F_c^2)^2/\Sigma w(F_o^2)^2]^{1/2}$.

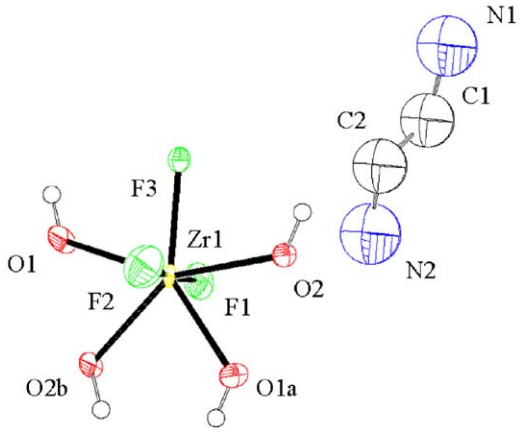

Fig. 4. ORTEP diagram and atom labeling scheme for SLUG-1.

Table 2
Bond lengths (Å) and angles (deg) for $[Zr(OH)_2F_3][enH]$

Zr1–F2	1.987(8)	Zr1–F1	2.030(7)
Zr1–F3	2.063(3)	Zr1–O2#1	2.133(3)
Zr1–O1#2	2.141(3)	Zr1–O2	2.149(3)
Zr1–O1	2.150(3)	Zr1–Zr1#2	3.5917(7)
Zr1–Zr1#1	3.5918(7)		
N1–C1	1.377(10)	C1–C2	1.518(9)
C2–N2	1.390(10)		
F2–Zr1–F1	177.32(16)	F2–Zr1–F3	88.3(6)
F1–Zr1–F3	89.1(5)	F2–Zr1–O2#1	93.9(4)
F1–Zr1–O2#1	88.6(4)	F3–Zr1–O2#1	142.05(10)
F2–Zr1–O1#2	92.5(3)	F1–Zr1–O1#2	89.2(3)
F3–Zr1–O1#2	141.58(12)	O2#1–Zr1–O1#2	76.25(12)
F2–Zr1–O2	88.3(4)	F1–Zr1–O2	90.4(4)
F3–Zr1–O2	75.81(11)	O2#1–Zr1–O2	142.08(10)
O1#2–Zr1–O2	65.83(12)	F2–Zr1–O1	96.5(3)
F1–Zr1–O1	83.5(3)	F3–Zr1–O1	76.14(12)
O2#1–Zr1–O1	65.96(12)	O1#2–Zr1–O1	141.60(14)
O2–Zr1–O1	151.35(15)	Zr1#1–O1–Zr1	113.67(15)
Zr1#2–O2–Zr1	114.03(14)	N1–C1–C2	114.2(11)
N2–C2–C1	106.1(11)		

Symmetry transformation codes: #1 $x+1/2,-y, z$ #2 $x-1/2, -y, z$.

Table 3
Hydrogen bond information for $[Zr(OH)_2F_3][enH]$ (Å and deg)

D–H···A	d(D–H)	d(H···A)	d(D···A)	∠(DHA)
O1–H1···F3#3	0.801(10)	1.946(18)	2.740(4)	170(10)
O2–H2···F3#4	0.799(10)	1.966(16)	2.742(4)	164(4)

D—donor atom, H—hydrogen, A—acceptor. Symmetry transformation codes: #3 $x+1/2, -y+1, z$ #4 $x-1/2, -y+1, z$.

fact the structure could also be synthesized using an equimolar amount of HF (48 wt% aqueous) as fluoride source. It is possible that higher dimensional materials may be possible by introducing a bridging group in some or all of these coordination positions. Indeed, our structure is quite similar to a $(CN_4H_7)ZrF_5$ pentagonal bipyramidal anionic chain reported previously [26], indicating that substitution of F by OH is possible. In the absence of the fluoride source, however, only an amorphous phase was obtained in initial experiments. Similarly, synthesis at higher temperature (>150 °C) or water content (>50H_2O:1 $Zr(O^nPr)_4$ mole ratio) only gave rise to a similar amorphous phase. Lower water content (< 20 H_2O:1 $Zr(O^nPr)_4$ mole ratio) did yield the product but larger amounts of the moisture-sensitive phase, as evidenced by reaction with the rinse water and concomitant reduced yield of the title compound (~23.2%).

Thermogravimetric analysis further supports the structural information obtained by XRD. The trace (Fig. 5) displays several thermal events. Physisorbed water is likely responsible for the weight loss up to ca. 160 °C, while the mass loss of ~14.6% from 160 °C through 200 °C corresponds to the loss of ca. one-third of the template

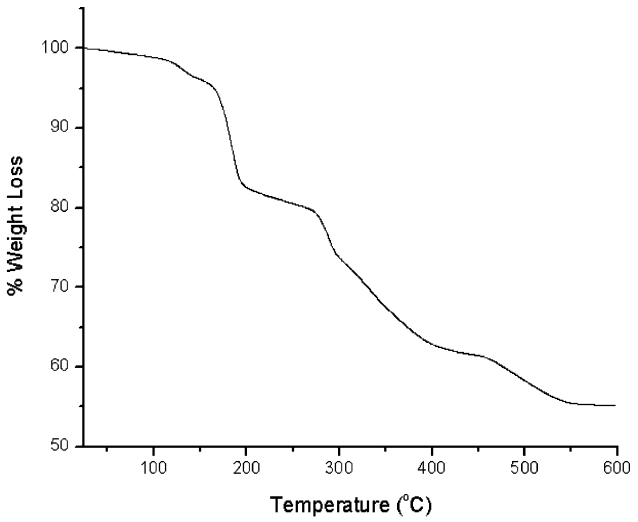

Fig. 5. TGA trace for the material, performed under nitrogen flow.

molecules and water from the condensation of the bridging hydroxide groups (theoretical: 15.3%). This behavior agrees with the elemental analysis performed on the material following heating to 230 °C, which showed the sample lost ~32% of the carbon and nitrogen present in the title compound. The loss of framework water over this temperature range is supported by literature data on zirconium fluoride compounds possessing hydroxide bridges [27]. In addition, the overall weight loss of 14.6% for this two-step process agrees well with the theoretical weight loss of 15.3%.

Interchain condensation can in some cases lead to a layered structure, for example, with aluminophosphates [28]. Chain-to-layer transformations are more likely when the chains are arranged in hydrogen-bonded layers [28], as is the case for the title compound.

Indeed, the appearance of strong 0 0 *l* PXRD reflections in Fig. 2b for the material heated to 230 °C (7.34, 3.72, and 2.49 Å, arising from the as-synthesized material's 0 0 2, 0 0 4 and 0 0 6 reflections, respectively) strongly implies that this intermediate is a layered compound. In addition, the weight loss plateaus in this region, also implying a stable intermediate. The crystallinity was unfortunately too low to determine the structure of this phase, even when the sample was slowly heated to this plateau region. Note, however, that the material is still open, with the (00*l*) peaks shifted to only slightly higher angle (Fig. 2b).

The next mass loss beginning at ~250 °C results from decomposition of the remaining organic constituents and loss of some fluoride. In agreement, the PXRD pattern for the bulk material heated to 400 °C (Fig. 2c) displays no peak below 20° (2θ) and matches the pattern for the condensed mineral phase $Zr(FO)_{2.7}$ (ICDD Card #39-1215) [29]. The observed 19.2% mass loss from this step agrees well with the expected loss of 19.7%. The transition results in a stoichiometric increase in oxygen, likely from the impure house nitrogen used as flow gas. This increase is not especially surprising due to the excellent oxygen-scavenging ability of zirconium [30]. The final transition is to the baddeleyite form of ZrO_2 (Fig. 2d, ICDD, Card #13-0307), with TGA confirming the loss of the remaining fluoride (experimental weight loss: 6.5%; theoretical: 6.6%).

4. Conclusions

In summary, a zirconium hydroxyfluoride chain structure has been synthesized from an alkoxide precursor. Initial attempts to use other organic mono- and di-amines in place of ethylenediamine have yet to yield any novel structures. Instead, poorly crystalline ZrO_2 has thus far been the sole product. The present structure represents one of a small class of low dimensionality zirconium-based materials, and is the first 1D zirconium hydroxyfluoride chain. Thermal data indicate transformation to an unknown layered structure, followed by collapse to a condensed mineral phase. Open 1D materials may therefore be a pathway to new 2D and 3D materials.

Acknowledgments

This work was supported by a National Science Foundation Career Award (DMR-0506279). We thank Paul Sideris and Professor Clare Grey, Department of Chemistry, State University of New York at Stony Brook, as well as Dr. Jürgen Schulte, Department of Chemistry, State University of New York at Binghamton, for help in collecting and interpreting NMR data. D.P. Brennan also acknowledges the National Science Foundation K-12 Fellowship Program (DGE-0086375) for financial support through a teaching fellowship.

References

[1] See for example C. Serre, F. Taulelle, G. Ferey, Solid State Sci. 3 (2001) 623–632.
[2] D. Wang, R. Yu, N. Kumada, N. Kinomura, Chem. Mater. 12 (2000) 956–960.
[3] E. Kemnitz, M. Wloka, S. Troyanov, A. Stiewe, Angew. Chem. Int. Ed. 35 (1996) 2677–2678.
[4] M. Wloka, S.I. Troyanov, E. Kemnitz, J. Solid State Chem. 135 (1998) 293–301.
[5] M. Wloka, S.I. Troyanov, E. Kemnitz, J. Solid State Chem. 149 (2000) 21–27.
[6] M. Catti, S. Stramare, R. Ibberson, Solid State Ionics 123 (1999) 173–180.
[7] M. Catti, A. Comotti, S. Di Blas, Chem. Mater. 15 (2003) 1628–1632.
[8] P. Benard, M. Louer, D. Louer, J. Solid State Chem. 94 (1991) 27–35.
[9] P. Benard-Rocherulle, J. Rius, D. Louer, J. Solid State Chem. 128 (1997) 295–304.
[10] R.E. Sykora, M. Ruf, T.E. Albrecht-Schmitt, J. Solid State Chem. 159 (2001) 198–203.
[11] E. Goreshnik, M. Leblanc, V. Maisonneuve, J. Solid State Chem. 177 (2004) 4023–4030.
[12] M. Hursthouse, K. Malik, J. Thomas, J. Chen, J. Xu, T. Song, R. Xu, Russ. Chem. Bull. 43 (1994) 1787.
[13] H.H.-Y. Sung, J. Yu, I.D. Williams, J. Solid State Chem. 140 (1998) 46–55.

[14] D. Wang, R. Yu, X. Xing, Y. Chen, Z. Guo, N. Kumada, N. Kinomura, M. Takano, Solid State Ionics 175 (2004) 751–754.
[15] B. Zhang, D.M. Poojary, A. Clearfield, Inorg. Chem. 37 (1998) 249–254.
[16] A.P. Rizzato, C.V. Santilli, S.H. Pulcinelli, Y. Messaddeq, A.F. Craievich, P. Hammer, J. Non-Cryst. Solids 348 (2004) 38–43.
[17] T.O. Salami, K. Marouchkin, P.Y. Zavalij, S.R.J. Oliver, Chem. Mater. 14 (2002) 4851–4857.
[18] D.T. Tran, P.Y. Zavalij, S.R.J. Oliver, Acta Crystallogr. E 58 (2002) m742–m743.
[19] T.O. Salami, P.Y. Zavalij, S.R.J. Oliver, J. Solid State Chem. 177 (2004) 800–805.
[20] D.T. Tran, P.Y. Zavalij, S.R.J. Oliver, J. Am. Chem. Soc. 124 (2002) 3966–3969.
[21] G.M. Sheldrick, XPREP, University of Göttingen, 1997.
[22] G.M. Sheldrick, Acta Crystallogr. A 46 (1990) 467–473.
[23] G.M. Sheldrick, SHELXL-97, University of Göttingen, 1997.
[24] I. Elder, C.-S. Lee, H. Kleinke, Inorg. Chem. 41 (2002) 538–545.
[25] P. Vaqueiro, A.M. Chippindale, A.R. Cowley, A.V. Powell, Inorg. Chem. 42 (2003) 7846–7851.
[26] B.V. Bukvetskii, A.V. Gerasimenko, R.L. Davidovich, Koord. Khim. 18 (1992) 576.
[27] H. Sutcliffe, A. Thornton, J. Fluorine Chem. 28 (1985) 171–182.
[28] S. Oliver, A. Kuperman, A. Lough, G.A. Ozin, Chem. Mater. 8 (1996) 2391–2398.
[29] R. Papiernik, B. Frit, B. Gaudreau, Rev. Chim. Miner. 23 (1986) 400.
[30] S.J. Clarke, K.A. Hardstone, C.W. Michie, M.J. Rosseinsky, Chem. Mater. 14 (2002) 2664–2669.